Original Article

Efficient and cost-effective differentiation of induced neural crest cells from induced pluripotent stem cells using laminin 211

Kazuma Takahashi*, Shizuka Aritomi, Fumie Honkawa, Sayaka Asari, Ken Hirose, Atsushi Konishi

Ajinomoto Co., Inc., 1-1 Suzuki-cho, Kanagawa, Kawasaki, 210-8681, Japan

A B S T R A C T

Introduction: Neural crest cells (NCCs) are cell populations that originate during the formation of neural crest in developmental stages. They are characterized by their multipotency, self-renewal and migration potential. Given their ability to differentiate into various types of cells such as neurons and Schwann cells, NCCs hold promise for cell therapy applications. The conventional method for obtaining NCCs involves inducing them from stem cells like induced pluripotent stem cells (iPSCs), followed by a long-term passage or purification using fluorescence-activated cell sorting (FACS). Although FACS allows high purity induced neural crest cells (iNCCs) to be obtained quickly, it is complex and costly. Therefore, there is a need for a simpler, cost-effective and less time-consuming method for cell therapy application.
Methods: To select differentiated iNCCs from heterogeneous cell populations quickly without using FACS, we adopted the use of scaffold material full-length laminin 211 (LN211), a recombinant, xeno-free protein suitable for cell therapy. After fist passage on LN211, iNCCs characterization was performed using polymerase chain reaction and flow cytometry. Additionally, proliferation and multipotency to various cells were evaluated.
Result: The iNCCs obtained using our new method expressed cranial NCC- related genes and exhibited stable proliferation ability for at least 57 days, while maintaining high expression level of the NCCs marker CD271. They demonstrated differentiation ability into several cell types: neurons, astrocytes, melanocytes, smooth muscle cells, osteoblasts, adipocytes and chondrocytes. Furthermore, they could be induced to differentiate into induced mesenchymal stem cells (iMSCs) which retain the essential functions of somatic MSCs.
Conclusion: In this study, we have developed novel method for obtaining high purity iNCCs differentiated from iPSCs in a short time using LN211 under xeno-free condition. Compared with traditional methods, like FACS or long-term passage, this approach enables the acquisition of a large amount of cells at a lower cost and labor, and it is expected to contribute to stable supply of large scale iNCCs for future cell therapy applications.

1. Introduction

In 1998, human embryonic stem cells (ESCs) were first established [1], followed by the successful generation of human induced pluripotent stem cells (iPSCs) in 2007 [2]. Since then, numerous studies have been conducted to uncover the pathogenesis of previously unexplained refractory diseases [3], develop novel treatments [4], elucidate disease etiology and harness their potential for regenerative medicine. For the application of iPSCs in regenerative medicine or cell therapy, it is crucial to obtain only target cells and eliminate unnecessary cells, as contamination with residual undifferentiated iPSCs can cause severe side effects [5]. Therefore, it would be particularly beneficial to have intermediate cells between iPSCs and the targeted differentiated cells that are free from iPSCs contamination, possess multiple differentiation potentials, and exhibit stable proliferation. High purity neural crest cell (NCC) [6] free from undifferentiated iPSCs is one of the promising candidates for cell therapy.

The neural crest, a transient structure that forms between the epidermal ectoderm and the neural plate during early vertebrate development [7], play significant important role in vertebrate evolution, often referred to as the "fourth germ layer" [8]. NCCs are a group of cells that migrate to various sites in the embryo after undergoing de-epithelialization from the neural crest and epithelial-mesenchymal transition, and differentiate into specific cell types depending on their location [9]. For instance, NCCs located in the dorsal neural tube differentiate into specialized axonal-origin cell types [10]. Cranial NCCs form the craniofacial structures of the head, including the skull's cartilage and bone tissue, cranial neurons, glia and facial connective tissue. Trunk NCCs differentiate into various cell types, including dorsal root ganglia that contain sensory neurons, satellite glial cells, adrenal gland endocrine cells and Schwann cells along spinal nerves [11]. Some of these NCCs differentiate into skin melanocytes and vagal NCCs form the enteric nervous system along the gut length [12], and contribute to the arteries' connective tissue, the outflow tract septum, and the cardiac ganglia [13].

NCCs were initially identified in rodents by Stemple and Anderson [14], who isolated these cells using cell sorting against the NCC-specific cell surface protein, p75NTR (neurotrophin receptor [NTR]). These p75NTR positive cells demonstrated self-renewal ability and generated both myofibroblasts and peripheral nervous system neurons and glia. Notably, since NCCs have been shown to be one of the originating cells of MSCs [15], which are frequently used in cell therapy, the generation of iMSCs from iPSCs via iNCCs lineage has been viewed as a promising approach in innovative medicine. To date, numerous studies have been conducted to establish a robust and efficient method for inducing iNCCs from ESCs/iPSCs [16–22]. The traditional method to purify iNCCs from heterogeneous cell populations is long-term passage [20] or fluorescence-activated cell sorting (FACS) [23]. The former method simply selects only robust and high growth iNCCs by long-passage, but is time-consuming and difficult to obtain high purity iNCCs. The latter method was first proposed as xeno-free method which can be useful for cell therapy and could dramatically shorten the period compared with the former method. The advantage of FACS method is to obtain high purity iNCCs, however several following bottlenecks must be improved for clinical use in near future: administrative costs of instrument, complexity of operation and limited processing capacity associated with the equipment used in cell processing facilities.

To overcome these issues, we have established a novel simple and cost-effective purification method by adapting scaffold material Laminin 211. This method simply utilizes Laminin 211 as a specific scaffold for selecting iNCCs from heterogeneous cell populations composed of undifferentiated iPSCs and some ectodermal cells. Additionally, the differentiation and purification processes are carried out under completely xeno-free conditions, which can be applied to cell therapy. Compared to the long-term passage method that takes approximately 4 weeks, a single passage on the scaffold is able to be performed in just 1 week and to enhance the purity of iNCCs. The cells obtained through this method retained their iNCC surface marker profiles even after 57 days and the obtained iNCCs successfully differentiated into various cell types, such as neurons, corneal endothelial cells and iMSCs.

2. Materials and methods

2.1. Cells and materials

iPSCs (201B7, 1210B2 and 1231A3) were obtained from iPS Portal Inc (Kyoto, Japan). The culture substrate used was 6-well plates (BD Biosciences, NJ, USA, 353046). As scaffolds, iMatrix-511 (Nippi, Tokyo, Japan, 892012; LN511-E8), Vitronectin-N (FUJIFILM Wako Pure Chemical, Osaka, Japan, 220-02041; VN), Laminin211 (Biolamina, Sundbyberg, Sweden, BLA-LN211-0; LN211) and Fibronectin (Sigma-Aldrich, MO, USA, F2006; FN) were used.

2.2. Induction and culturing of iNCCs from iPSCs

The differentiation of iNCCs from iPSCs was carried out following previously reported methods [16,23]. Initially, iPSCs were seeded in a 6-well plate with a density of 6500 cells/well in a 1.5 mL suspension of StemFit® AK03 N (Ajinomoto, Tokyo, Japan) mixed with 4.8 µL LN511-E8. After five days of cultivation, the medium was switched to iNCC induction medium: StemFit Basic03 (Ajinomoto) containing 0.6 µM CHIR99021 (FUJIFILM Wako Pure Chemical, 038-23101; CHIR) and 10 µM SB431542 (Reprocell, Kanagawa, 04-0010). The medium was changed every two days, and the cells were cultured for 14 days to induce iNCCs. Following induction, colonies obtained were dissociated into single cells using a cell detachment solution: TrypLE™ Select CTS™ (Thermo Fisher Scientific, MA, USA, A12859-01) containing 50 U/mL DNase (QIAGEN, Venlo, Nederland, 79254). These cells were then cultured and maintained in iNCC maintenance medium: StemFit Basic03 containing 10 µM SB431542, 20 ng/mL Epidermal Growth Factor (Sigma-Aldrich, MO, USA, E9644), 20 ng/mL CORYNEX® basic FGF (Ajinomoto) and 0.4 µL/mL LN211 for a week. Medium exchanges were performed every 2–3 days. During long-term maintenance culture experiments, cells were passaged every 3–7 days once they reached 80% confluency. In this study, scaffolds were added to the medium during the culture of iPSCs and the purification and expansion culture of iNCCs. This approach has been shown to achieve the same effect as coating with scaffolds, as reported in previous studies [24].

2.3. Differentiation of iNCCs

2.3.1. Neuron differentiation

Cells were suspended at a concentration of 2×10^4/150 µL in iNCC maintenance medium and seeded onto Sumitomo PrimeSurface U (Sumitomo Bakelite, Tokyo, Japan) to form spheres after 24 h. The spheres were seeded onto Poly-ornithine and mouse Laminin-coated 48-well plates and cultured for 9 days in Neurobasal medium (Thermo Fisher Scientific, 21103049) supplemented with 2% B27 (Thermo Fisher Scientific, 12587010), 5 ng/mL BDNF (Peprotech, NJ, USA, 450-02-10UG), 10 ng/mL GDNF (Peprotech、450-10-10UG), 400 µM dbcAMP (Nacalai Tesque, Kyoto, Japan, 11540-74) and 200 µM ascorbic acid (FUJIFILM Wako Pure Chemical, 012-04802). After the culture period, cells were fixed with 4% paraformaldehyde (PFA) (Nacalai Tesque, 09154-85) for

immunostaining. Nuclei were stained with Cellstain®- Hoechst 33342 solution (DOJINDO, 346-07951; Hoechst) and the antibodies used are listed in Table 1.

2.3.2. Astrocyte (Schwann cell) differentiation

Cells were seeded onto Poly-ornithine and Laminin-coated 24-well plates at a density of $2.5 \times 10^4/cm^2$ and cultured for 10 days in DMEM/F12 (Thermo Fisher Scientific, 11330-032) supplemented with 1% N2 supplement (Thermo Fisher Scientific, 17502), 2 mM GlutaMAX-I supplement (Thermo Fisher Scientific, 35050) and 1% fetal bovine serum (Thermo Fisher Scientific, 26140-079; FBS). After the culture period, cells were passaged, fixed the next day with 4% PFA, and used for immunostaining. Nuclei were stained with Hoechst and the antibodies used are listed in Table 1.

2.3.3. Melanocyte differentiation

Cells were seeded onto fibronectin-coated 24-well plates at a density of $1.25 \times 10^4/cm^2$ and cultured in DMEM/F12 supplemented with 20% StemFit for Differentiation (Ajinomoto), 1 μM CHIR, 25 ng/mL BMP4 (R&D SYSTEM, MN, USA, 314-BP-050) and 100 nM Endothelin-3 (Peptide institute, Ibaraki, Japan, 4199-v). After 3 days, cells were passaged and cultured for an additional 7 days, then fixed with 4% PFA and used for immunostaining. Nuclei were stained with Hoechst and the antibodies used are listed in Table 1.

2.3.4. Smooth muscle cell differentiation

Cells were seeded onto 24-well plates at a density of $1.25 \times 10^4/cm^2$ and cultured in αMEM (Nacalai Tesque, 21444-05) supplemented with 10% FBS. After being passaged twice at sub-confluence, cells were fixed with 4% PFA for immunostaining. Nuclei were stained with Hoechst and the antibodies used are listed in Table 1.

2.3.5. Osteoblast differentiation

Cells were suspended in iNCC maintenance medium at a concentration of $2 \times 10^4/500$ μL and seeded onto 24-well plates. When cells reached 60% confluence, they were cultured in DMEM-HG (Thermo Fisher Scientific, 11965092) supplemented with 10 mM β-glycerol phosphate (Nacalai Tesque, 1713022), 100 nM dexamethasone (FUJIFILM Wako Pure Chemical, 047-18863; Dex) and 50 μM ascorbic acid for 31 days, then fixed with 4% PFA and stained with Alizarin Red S (Nacalai Tesque, 01303-52) staining.

2.3.6. Adipocyte differentiation

Cells were suspended in iNCC maintenance medium at a concentration of $3 \times 10^4/500$ μL and seeded onto 24-well plates. When cells reached 60% confluence, they were cultured in DMEM-HG supplemented with 100 nM Dex, 500 μM isobutylmethylxantine (FUJIFILM Wako Pure Chemical, 099-03411) and 50 μM indomethacin (Sigma-Aldrich, I7378) for 31 days, then fixed with 4% PFA and stained with Oil Red O (Sigma-Aldrich, O0625) staining.

2.3.7. Chondrocyte differentiation

Cells were suspended in DMEM-HG supplemented with 100 nM Dex, 50 μM Ascorbic Acid, ITS liquid supplement (Sigma-Aldrich, I3146), 1 mM Sodium Pyruvate (Nacalai Tesque, 06977-34), 10 ng/mL TGF-β1 (Peprotech, 100-21C) and 50 μg/mL L-proline (Sigma-Aldrich, P5607) at a concentration of $2.5 \times 10^4/500$ μL and seeded onto 24-well plates. After 33 days of culture, cells were fixed with 4% PFA and stained with Alcian blue (FUJIFILM Wako Pure Chemical, 015-13805) staining.

2.3.8. iMSC differentiation

Cells were seeded onto 6-well plates coated with 1.5 μg/cm^2 VN at a density of 1×10^5 cells/well for proliferation and maintained in iMSC medium; StemFit for Mesenchymal Stem Cell (Ajinomoto) with 90 nM dexamethasone. iMSC was induced by cultivation for 12—14 days with medium change in every 2—3 days and passage in every 4—5 days. The same procedure was followed for long-term maintenance culturing of iMSCs however, medium change was conducted every 2—3 days, and passage was performed every 5—7 days.

2.4. Differentiation of iMSCs

2.4.1. Osteoblast differentiation

Cells were suspended in iMSC medium at a concentration of 2×10^4 cells/500 μL and seeded onto 24-well plates coated with VN. After reaching 60% confluence, the cells were cultured for 41 days in DMEM-HG supplemented with 10% FBS, 10 mM β-glycerol phosphate, 100 nM Dex and 50 μM ascorbic acid. The cells were fixed with 4% PFA and subjected to Alizarin Red S staining.

2.4.2. Adipocyte differentiation

Cells were suspended in iMSC medium at a concentration of 3×10^4 cells/500 μL and seeded onto 24-well plates coated with VN. At 60% confluence, the cells were cultured for 38 days in DMEM-HG supplemented with 10% FBS, 100 nM Dex, 500 μM iso-butylmethylxanthine and 50 μM indomethacin. The cells were fixed with 4% PFA and subjected to Oil Red O staining.

2.4.3. Chondrocyte differentiation

Cells were suspended in DMEM-HG supplemented with 10% FBS, 100 nM Dex, 50 μM ascorbic acid, 1% N-2 Supplement, 1 mM Sodium Pyruvate, 10 ng/mL TGF-β1 and 50 μg/mL L-proline at a concentration of 2.5×10^4 cells/500 μL and seeded onto 24-well plates. After 44 days of culture, the cells were fixed with 4% PFA and subjected to Alcian blue staining.

2.5. Inflammatory response of iMSCs

iMSCs were suspended in iMSC medium and seeded onto 6-well plates coated with VN at a density of 3.0×10^4 cells/well. When they reached 80% confluence, 50 ng/mL of Interferon γ (R&D

Table 1
Antibody list for iNCC differentiation ability test.

Cell	Primary antibody	Secondary antibody	Tertiary antibody
Astrocyte	Anti-GFAP antibody (abcam, ab7260)	Goat anti-Rabbit IgG (H + L) Cross-Adsorbed Secondary Antibody, Biotin-XX (Thermo Fisher, B-2770)	Streptavidin, Alexa Fluor™ 488 conjugate (Thermo Fisher, S11223)
Melanocyte	Anti-MiTF antibody [C5] (abcam, ab12039)	Goat anti-Mouse IgG (H + L) Cross-Adsorbed Secondary Antibody, Biotin-XX (Thermo Fisher, B-2763)	
Neuron	Anti-Tubulin Antibody, beta III isoform, CT, clone TU-20 (Millipore, MAB1637)	Anti-mouse IgG (H + L), F(ab')2 Fragment (Alexa Fluor® 555 Conjugate) (Cell Signaling, 4409S)	—
Smooth muscle cell	Anti-Actin, α-Smooth Muscle antibody, Mouse monoclonal (Sigma, A5228-100UL)		

Systems, 285-IF-100; IFNγ) was added, and the cells were further cultured for 48 h. Additionally, BM-MSCs (Lonza, Basel, Switzerland, PT-250) cultured in StemFit for Mesenchymal Stem Cell containing 0.2 μg/mL LN511-E8 were used as controls.

2.6. Immunosuppressive effect of iMSCs

To evaluate the ability of iMSCs to inhibit the proliferation of peripheral blood mononuclear cells (Lonza, CC-2702; PBMCs), BM-MSCs and iNCCs were used as a positive control and a negative control, respectively. These cells were seeded onto a 96-well plate coated with VN (0.5 μg/cm^2) at a density of 5×10^4/well (n = 3) in their respective growth medium. The day after seeding, the medium was replaced with 100 μL/well of RPMI supplemented with GlutaMAX-I ($1 \times$) (Thermo Fisher Scientific, 61870-036; RPMI), 2.5 μg/mL Mitomycin C (Nacalai Tesque, 20898-21), 10% FBS, and the cells were treated for 1 h at 37 °C. After washing twice with PBS (Nacalai Tesque, 14249-24), the medium was switched to RPMI supplemented with 10% FBS, and 1×10^5/well PBMCs along with the stimulant, 2.5 μL/well of Dynabeads Human T-Activator CD3/CD28 (Thermo Fisher Scientific, 11131D) and 30 U/mL Interleukin-2 human (Sigma-Aldrich, 11011456001), were added and incubated at 37 °C. Cell proliferation of PBMCs was evaluated by the absorbance measured using Cell Proliferation ELISA, BrdU (colorimetric; Sigma-Aldrich, 11647229001) three days after co-culturing.

2.7. Flow cytometric measurement (FCM)

For the analysis of MSC surface markers, cells were incubated at room temperature for 10 min in Human TruStain FcX™ (Biolegend, CA, USA, 422301) diluted 50 times with PBS. Afterward, an antibody solution diluted 10 times with FCM buffer: PBS with 1% FBS was added and incubated on ice and in the dark for 20 min. After washing three times with FCM buffer, the cells were suspended in Attune 1x focusing fluid (Thermo Fisher Scientific, A24904), and analysis was performed using the Attune NxT Flow Cytometer (Thermo Fisher Scientific). To analyze IDO's stimulus responsiveness, cells were fixed with 4% PFA at room temperature for 30 min. Then the cells were blocked with Blocking One Histo (Nacalai, 06349-64) at room temperature for 60 min and treated with a primary antibody diluted 20 times for 30 min on ice, followed by a secondary antibody diluted 500 times in the dark on ice for 30 min before measurement. The antibodies used are listed in Table 2. During measurement, the laser intensity was adjusted so that the fluorescence intensity of the cells stained with the isotype control was below 10^3. Cell populations showing fluorescence intensity above 10^3 were defined as positive cells, and specifically, above 10^4 were defined as high-expression populations. From this point

forward, cells with high expression of CD271 will be referred to as CD271^{high} cells.

2.8. Gene expression analysis

The cells to be analyzed were stored at −80 °C in Buffer RLT Plus (QIAGEN, 1053393), and RNA was extracted using the RNeasy Plus mini kit (QIAGEN, 74134). cDNA was synthesized using SuperScript VILO MasterMix (Thermo Fisher Scientific, 11756050). RealTime-PCR was performed using the TaqMan™ Gene Expression Master Mix (Thermo Fisher Scientific, 4369016) for the Taqman probe and the Fast SYBR Green Master Mix (Thermo Fisher Scientific, 4385612) for other synthetic primers. The list of used Taqman probes and synthetic primers are shown in Table 3. The expression levels of each gene were normalized by the expression level of the housekeeping gene, β-actin (ACTB). Subsequently, the values corresponding to the gene expression levels in undifferentiated iPSCs (201B7) were charted on a graph.

2.9. Statistical analyses

All statistical analyses were performed using the GraphPad Prism10 software (GraphPad Software Inc., CA, USA). For comparisons between two groups, an unpaired *t*-test was used. For comparions involving more than two groups, a two-way ANOVA followed by Bonferroni's post hoc test was conducted. Statistical significance was indicated as follows: *$p<0.05$, **$p<0.01$, ***$p<0.001$, ****$p<0.0001$. Data are presented as means ± SD, and the number of replicates (n) is specified in the figure legends.

Table 3
List of Taqman probes and synthetic primers.

Taqman probe	
Target gene	Primer ID
ACTB	Hs01060665_g1
SOX10	Hs00366918_m1
TFAP2A	Hs01029413 _ m1
SOX9	Hs01001343_g1
TWIST1	Hs01675818_s1
OTX2	Hs00222238_m1

Synthetic primer		
Target gene	Forward	Reverse
ACTB	CATAGTCCGCCTAGAAGC	GTTGCTATCCAGGCTGTG
OCT3/4	CCTCACTTCACTGCACTGTA	CAGGTTTTCTTTCCCTAGCT
DLX1	CGACCTTCAGCTTTGTGGGACTA	GACGGATGAGGACCTGGACTTTAC
HOXA2	ATTGTCATTGGGCAGAAGCA	GGACCGCGCTACTATTAAACTATTG
HOXA3	GGATGCTTCGCGGTCTGTTA	CTCCGTTTGCTGGAGACCTG

Table 2
List of antibodies for FCM.

Marker	Primary antibody	Secondary antibody	Isotype Control
NCC	PE Mouse Anti-Human CD271 (BD, 557196)	−	PE Mouse IgG1, kappa Isotype Ctrl (Biolegend, 400139)
MSC positive	PE anti-human CD105 Antibody (Biolegend, 323205)	−	
MSC negative	PE anti-human CD34 Antibody (Biolegend, 343605)	−	
MSC positive	FITC anti-human CD73 (Biolegend, 344016)	−	FITC Mouse IgG1, kappa Isotype Ctrl (Biolegend, 400110)
MSC positive	FITC anti-human CD90 (Thy1) Antibody (Biolegend, 328107)	−	
MSC negative	FITC anti-human CD45 (Biolegend, 304005)	−	
MSC positive	APC anti-human CD44 Antibody (Biolegend, 338805)	−	APC Mouse IgG2a, κ Isotype Control (BD, 555576)
Pharmacological activity	Human Indoleamine 2,3-dioxygenase/IDO Antibody (R&D, MAB6030)	Goat anti-Mouse IgG (H + L) Highly Cross-Adsorbed Secondary Antibody, Alexa Fluor™ 488 (Thermo Fisher, A11029)	Purified Mouse IgG1, kappa Isotype Ctrl (Biolegend, 401401)

3. Results

3.1. Optimization of iNCC induction and purification methods

First of all, the induction method for iNCCs from iPSCs was optimized, with reference to previous reports [16,23]. iPSCs were cultivated with StemFit AK03 N for 5 days, followed by iNCC induction for 14 days with StemFit Basic03 supplemented with CHIR99021 (CHIR). Subsequently, iNCCs were purified from heterogeneous colonies. (Fig. 1A). For effective iNCC induction, the concentration of CHIR at the induction stage is crucial [16], therefore the concentration of CHIR during differentiation was optimized for the cell line, 201B7. To evaluate iNCC differentiation efficiency, CD271 was adopted as a marker, which is highly expressed in NCCs
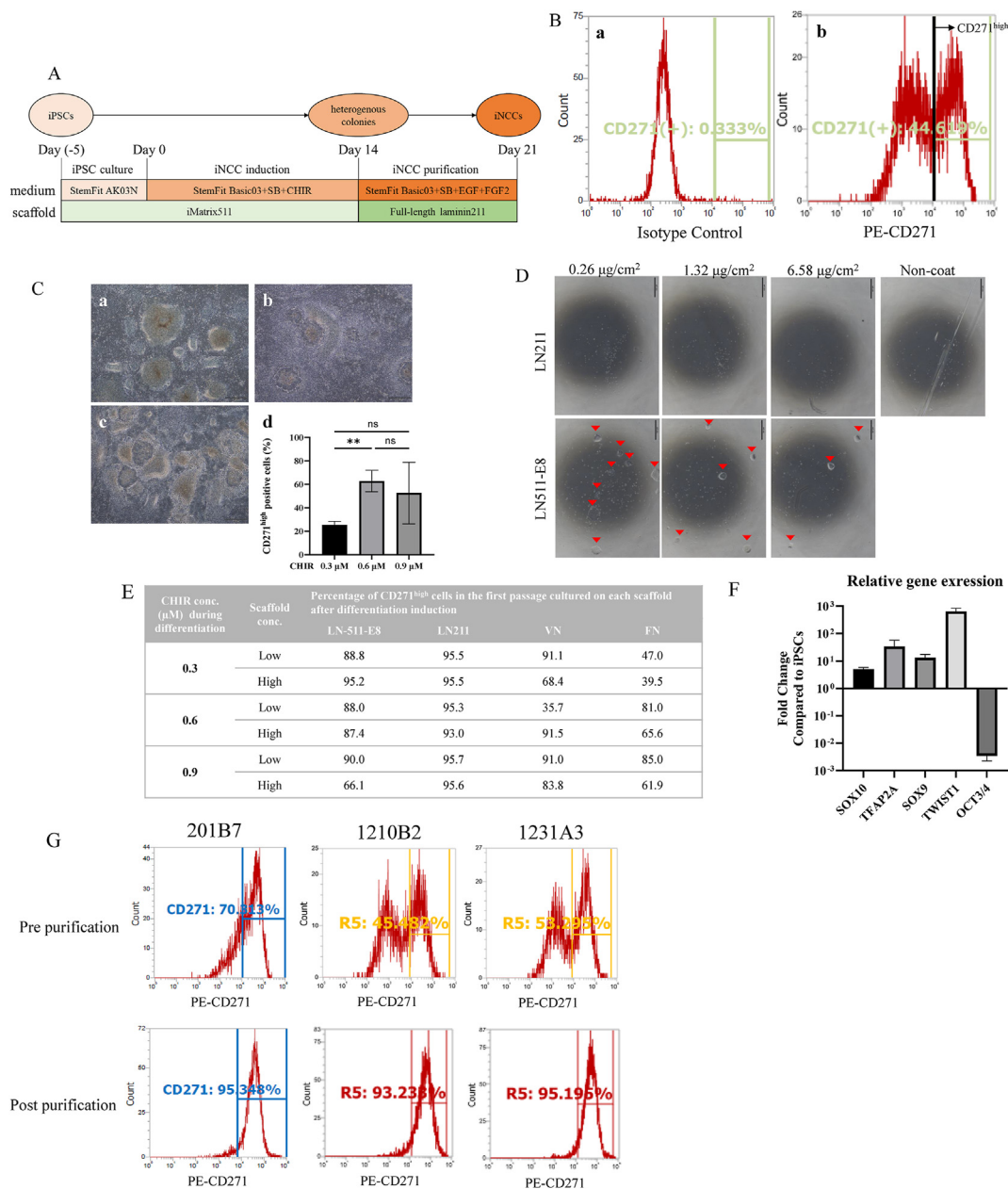

Fig. 1. Optimization of iNCCs induction and purification methods. A. The diagram illustrates the iNCC induction and purification method. SB, SB431542. CHIR, CHIR99021. B. The histogram represents the results from flow cytometry measurements of the heterogeneous cell population following NCC induction, stained with isotype control (a) or CD271 antibody (b). Among the CD271 positive cells, the populations with a fluorescence intensity of 10^4 (marked with a line) or higher were defined as high CD271 expression (CD271^{high}) cells. C. Morphology of colonies on day 14 when iNCCs were induced from iPSCs under various CHIR concentrations (0.3 μM (a), 0.6 μM (b), 0.9 μM (c)), along with the percentage of CD271^{high} cells induced at each concentration (d). Statistical significance was determined using an unpaired t-test. *$p<0.05$. Data are represented as the mean ± SD, n = 3. Scale Bar: 500 μm. D. Representative microscopic images of iPSCs (201B7) cultured in StemFit AK03 N supplemented with either LN211 or LN511-E8 at their respective concentrations. Arrowheads indicate the colonies. Scale Bar: 500 μm. E. The percentage of CD271^{high} cells in the first passage after culture with each scaffold. The low dose of LN511-E8, LN211, and VN was 0.6 μL/mL, and the high dose was 6 μL/mL. The low dose of FN was 15 μL/mL, and the high dose was 30 μL/mL. F. The relative gene expression of NCC Marker Genes (SOX10, TFAP2A, SOX9, TWIST1) and pluripotency marker (OCT3/4) in iNCCs purified using LN211 compared with the expression of iPSCs (201B7). The expression levels of each gene were normalized by that of the housekeeping gene, β-actin (ACTB). Data are represented as the mean ± SD, n = 3. G. The histograms display the results from flow cytometry measurements of various iPSC-derived cells pre (upper) and post (lower) iNCCs purification (left: 201B7, middle: 1210B2, right: 1231A3). Cell populations with a fluorescence intensity of 10^4 or above (the right side of the vertical line) are classified as CD271^{high} cells. The data were obtained with N = 1.

[14,25] along with other NCC marker proteins. Since the expression level per cell is important for the quality of iNCCs, we have defined a suitable CD271 expression level for functional iNCCs as CD271^{high} by flow cytometry (Fig. 1B). At the day 14 of iNCC differentiation, heterogenous colonies were observed among all CHIR concentrations (Fig. 1C a, b, c). Among three concentrations 0.6 μM of CHIR consistently showed a higher population of CD271^{high} cells compared to 0.3 μM (Fig. 1C d), although no significant difference was observed between 0.3 μM and 0.9 μM or between 0.6 μM and 0.9 μM. Therefore, the CHIR concentration was set at 0.6 μM in this study.

Secondly, the iNCC purification method was investigated. Since it was reported that the usage of laminin211-E8 fragment (LN211-E8) could enhance efficiency of differentiation from iPSCs to iNCCs when used as a scaffold [26], it was hypothesized to be beneficial for the purification of iNCCs. However, it was deemed unsuitable due to it reports indicating its support for iPSCs proliferation [26]. Given the lower growth supportive ability of full-length laminin211 (LN211) to iPSCs compared to that of LN211-E8 while that to iNCCs are still retained by LN211, LN211 may possess the potential for purification of iNCCs in the post-differentiation stage. In order to clarify the growth-supportive ability of LN211, iPSCs were cultured either on LN511-E8 or LN211 for 5 days, and iPSCs colony formation was observed on LN511-E8 at all concentrations, while LN211 was not (Fig. 1D). This suggests that, unlike LN211-E8 as shown in the previous report [26], LN211 cannot support proliferation of iPSCs. Furthermore, this presents the possibility of it being a scaffold for purification.

To evaluate the potential applicability of LN211 for iNCC purification, the ability to isolate iNCCs was examined in comparison with other commonly used scaffolds. During the differentiation stage, iPSCs were cultured with three different concentrations of CHIR on scaffold, LN511-E8 for 14 days. The obtained colonies, comprised of iNCCs and iPSCs, were enzymatically dissociated into single cells and subsequently seeded on various scaffolds, including LN211, at both low and high concentrations in the iNCC maintenance medium. Among all scaffolds, LN211 showed the highest population of CD271^{high} regardless of its coating concentrations and even when the CHIR concentration was not optimal (Fig. 1E).

The gene expression patterns of the CD271^{high} cells obtained using LN211 were investigated to determine whether they possess characteristics of NCCs, as opposed to those of iPSCs. In comparison to the undifferentiated state, the expression of NCC markers TFAP2a, SOX9, SOX10 and TWIST1 was elevated, while the expression of OCT3/4, an undifferentiated marker for iPSCs, significantly decreased (Fig. 1F). Consequently, the usage of LN211 was considered to be the optimal purification scaffold for obtaining high-purity iNCCs without the need for long-term passage. In addition to 201B7 cell line, iNCC differentiation and purification with LN211 was investigated using 1210B2 and 1231A3 cell lines, with a significant increase in the CD271^{high} population observed post purification across all cell lines (Fig. 1G).

3.2. Investigating the characteristic of iNCCs obtained using established methods

The self-renewal and multilineage capacities of the obtained iNCCs using newly established method with LN211were examined, given that NCCs typically possess these abilities [27]. In terms of self-renewal ability, the iNCCs were cultured for 57 days with iNCC maintenance medium, exhibiting an approximate population doubling level (PDL) of 36 while maintaining CD271^{high} profiles (Fig. 2A).

Prior to assessing the multilineage capacity, in order to ascertain whether the obtained iNCCs exhibit embryological character of NCC, using cells post the first passage on LN211 were analyzed for the expression of NCC marker genes, including OTX2 for the mesencephalon [28], Dlx1 for the first (maxillary) and second (lingual) pharyngeal arches [29], and HOXA2 and HOXA3 for the second and third (thymus) pharyngeal arches [30,31] (Fig. 2B). Only Dlx1, the marker for the first and second pharyngeal arches, exhibited significantly high expression (Fig. 2C).

The multilineage capacity of the iNCCs was also substantiated. Generally, migrating NCCs from the first and second pharyngeal arches have the potential to differentiate into variety of the cell types, including neurons, Schwann cells, melanocytes, smooth muscle cells, osteoblasts, adipocytes and chondrocytes. Prior studies have indicated that iNCCs, which exhibit characteristics resembling those of the first and second pharyngeal arches as in this study, capable of differentiating into the aforementioned cell types [16]. In order to substantiate the potential for differentiation into these cell types, differentiation inductions were performed using the iNCCs procured in this study. As a result, the cells post each induction were found to express TUJ1 (neurons; Fig. 2D a), GFAP (astrocytes; Fig. 2D b), MiTF (melanocytes; Fig. 2D c) and αSMA (smooth muscle cells; Fig. 2D d). Furthermore, adipocytes, osteoblasts and chondrocytes were stained with Oil Red O (Fig. 2D e), Alizarin Red (Fig. 2D f) or Alcian Blue, respectively (Fig. 2D g). These findings corroborated the multipotency of the iNCCs in this study.

3.3. Induction and functional verification of iMSCs from iNCCs obtained with LN211

Finally, the ability of the obtained iNCCs into iMSCs and their functional characteristics were investigated. Although MSCs are beneficial for cell therapy [32—36], somatic MSCs suffer from a lack of sufficient donor cells, and the proliferative and differentiation capacities of MSCs vary depending on the donor [37]. To address this issues, various methods for inducing iMSCs from iNCCs have been established [16,19,21—23,38—41]. iNCCs obtained in this study were cultured in StemFit for Mesenchymal Stem Cell supplemented with dexamethasone [41] for a period of 12 days.

MSCs are defined by International Society of Cell & Gene Therapy (ISCT) as cells that i) adhere to plastic under standard culture conditions, ii) express specific surface markers and iii) possess the capacity to differentiate into tri-lineages: osteoblasts, adipocytes and chondrocytes [42]. To confirm criterion i), the cells were cultured on a plastic dish where they exhibited stable cell proliferation for a duration of 57 days, demonstrating a finite proliferative capacity akin to that of somatic MSCs (Fig. 3A). To validate criterion ii), the expression of surface marker proteins was analyzed, revealing significant expression of CD44, CD90, CD73 and CD105, and negative expression of CD34 and CD45, thereby demonstrating the expression pattern characteristic of MSCs defined by ISCT. (Fig. 3B). To validate criterion iii), the cells obtained were subjected to differentiation induction towards the lineages previously mentioned. The results indicated significant stain with Oil Red O (adipocytes; Fig. 3C a), Alizarin Red (osteoblasts; Fig. 3C b), and Alcian Blue (chondrocytes; Fig. 3C c). This effectively confirmed their capacity for tri-lineage differentiation. Given that they fulfill all three criteria for MSCs, it could be inferred that the cells obtained may be iMSCs. Additionally, it was elucidated that the iNCCs obtained in this study also potentially possess the capability to differentiate into iMSCs.

Then the functionality of the iMSCs obtained in this study, in comparison with somatic MSCs was scrutinized. In order to validate inflammatory response, both iMSCs and BM-MSCs,
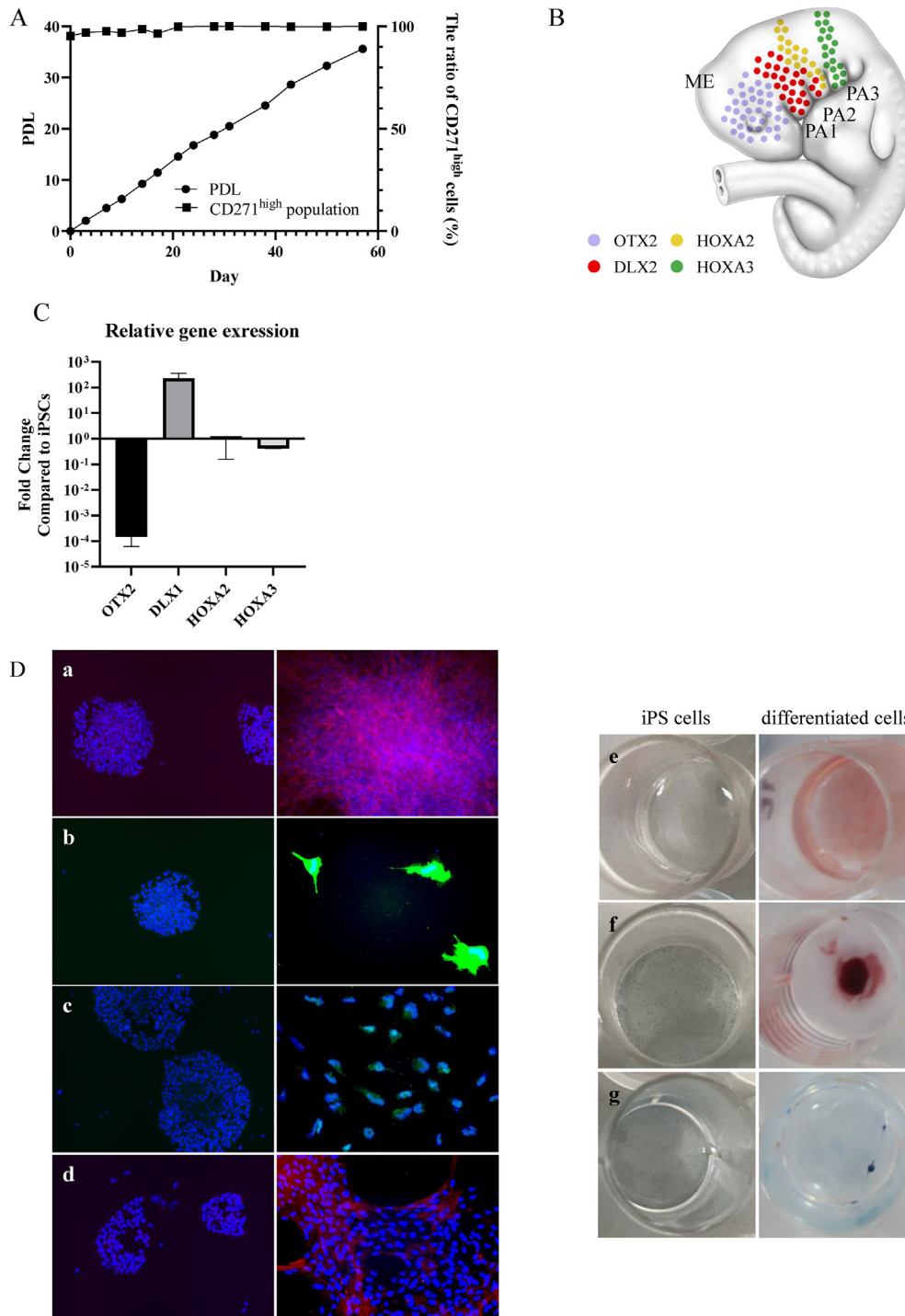
Fig. 2. Characteristics of iNCCs obtained with LN211. A. The self-renewal ability of iNCCs maintained in culture with LN211. The left axis shows the Population Doubling Level (PDL) in cell proliferation, while the right axis shows the percentage of CD271^{high} cells determined by flow cytometry measurements. B. The map displays the distribution of marker-positive cells in a human fetus at 4 weeks. ME, mesencephalon; PA1 to PA3, pharyngeal arch 1 to pharyngeal arch 3. C. The relative gene expression of NCC site-specific marker in iNCCs purified using LN211 compared with iPSCs (201B7). The expression levels of each gene were normalized by that of ACTB. Data are represented as the mean ± SD, n = 3. D. Staining images of cells post-differentiation induction and iPSCs (201B7): (a) Neuron (Red: TUJ1, Blue: Hoechst), (b) Astrocyte (Green: GFAP, Blue: Hoechst), (c) Melanocyte (Green: MiTF, Blue: Hoechst), (d) Smooth Muscle Cell (Red: αSMA, Blue: Hoechst), Tri-lineage (Osteoblast, Adipocyte, Chondrocyte): (e) Oil Red O Staining (Red: Adipocyte) (f) Alizarin Red Staining (Deep Red: Osteocyte) (g) Alcian Blue Staining (Blue: Chondrocyte).

serving as the positive control for somatic MSCs were stimulated with IFNγ. It was observed that iMSCs, akin to BM-MSCs exhibited an increase in IDO (indoleamine 2,3-dioxygenase) protein expression (Fig. 3D). To assess the immunosuppressive effect of iMSCs, PBMCs (peripheral blood mononuclear cells) stimulated with CD3/CD28/IL-2 were co-cultured with either iMSCs or BM-MSCs, or with iNCCs serving as a negative control. Contrary to iNCCs, which failed to inhibit the proliferation of CD3/CD28/IL-2-stimulated PBMCs, iMSCs effectively suppressed growth in a manner akin to BM-MSCs (Fig. 3E a). Furthermore,
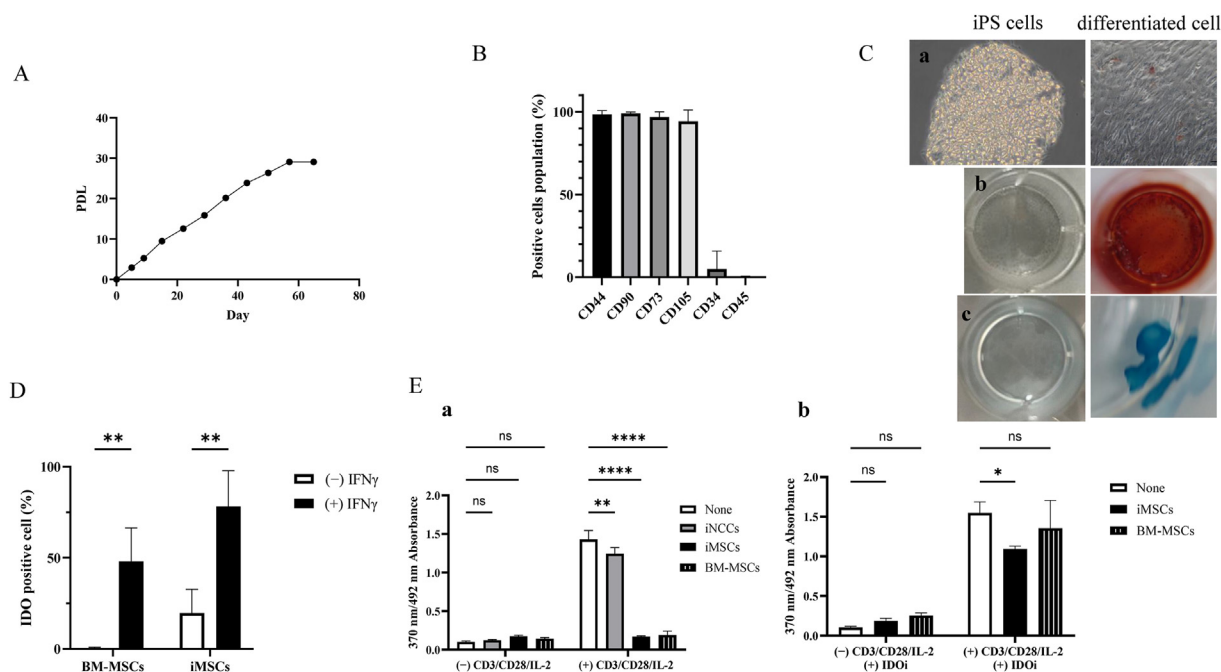
Fig. 3. Induction and functional verification of iMSCs from iNCCs obtained with LN211. A. PDL of iMSCs maintained under xeno-free culture conditions. B. The percentage of MSC definition marker proteins positive cells at the end of iMSC induction, measured by flow cytometry. CD44, CD90, CD73 and CD105 are positive markers, and CD34 and CD45 are negative markers for MSCs. Data are presented as the mean ± SD, n = 3. C. Staining images of cells post-differentiation induction and iPSCs (201B7): Tri-lineage differentiation potential of iMSCs (Adipocyte (a), Osteoblast (b), Chondrocyte (c)). D. The percentage of IDO protein positive cells with and without IFNγ stimulation for 48 h, measured by flow cytometry. Statistical significance was determined using a two-way ANOVA followed by Bonferroni's post hoc test. **p<0.01. Data are represented as mean ± SD, n = 3. E. PBMC proliferation when co-cultured with iNCCs, iMSCs and BM-MSCs was measured under conditions with and without CD3/CD28/IL-2 stimulation (a). In addition, for iMSCs and BM-MSCs, PBMCs proliferation was determined in the presence of an IDO inhibitor (IDOi) (b). Cell proliferation was evaluated based on absorbance using a Cell Proliferation ELISA BrdU Kit. This assay measures the incorporation of BrdU, a thymidine analog, during cell division by reacting it with peroxidase-conjugated anti-BrdU antibodies and detecting at an absorbance of 370 nm. A correction was made using the absorbance at 492 nm. The y-axis of the graph represents the amount of incorporated BrdU, which is proportional to cell proliferation. Statistical significance was determined using a two-way ANOVA followed by Bonferroni's post hoc test. *p<0.05, **p<0.01, ****p<0.0001. Data are presented as the mean ± SD, n = 3.

the effect of suppressing cell proliferation was nullified with the introduction of IDO inhibitors (Fig. 3E b). The observations imply that the iMSCs acquired in this study suppress the proliferation of PBMCs by the same mechanism as somatic MSCs.

4. Discussion

In this study, we pioneered the utilization of LN211 as a purification scaffold, thereby establishing a straightforward method to derive high-purity iNCCs from a heterogeneous population comprising iNCCs and iPSCs within a limited time frame (Fig. 1A). In comparison to the conventional long-term passage method, the purification process was significantly condensed from approximately 4 weeks to 1 week. Moreover, in comparison to the FACS method, our innovative method does not necessitate expensive equipment or intricate operations, thereby significantly mitigating costs. Previous methodologies [16,20] have incorporated animal-derived materials during iNCC differentiation, which restricts their clinical application due to potential immunogenicity and risk of disease transmission [43,44]. The methodology established in this study circumvents the utilization of animal-derived materials during both the differentiation and purification phases, thereby augmenting the potential of iNCCs as a source for cell therapies.

Full-length laminin211 (LN211) has the capability to selectively isolate CD271^{high} cells from a heterogenous cell population, which includes iNCCs, iPSCs and an assortment of differentiated cells. A prior study proposed the laminin211-E8 fragment (LN211-E8) as an appropriate scaffold for iNCC induction. However, it was also

observed to support proliferation of undifferentiated iPSCs [45], indicating a necessity for enhanced specificity in iNCC isolation. To eliminate growth-supportive ability to iPSCs, we utilized LN211 instead of LN211-E8 in this research. Laminin-E8 is a fragment where the integrin binding site found in the full-length is entirely preserved, and other areas such as heparin/heparan sulfate binding are excised [46,47]. It has been documented that the cell adhesion and proliferative capacity of iPSCs cultivated with the laminin511-E8 fragment surpassed those cultivated with the full-length laminin511 [48]. Consequently, the cell growth-supportive ability of LN211 to undifferentiated iPSCs might be inferior to that of LN211-E8. In our study, iPSC cultivation on LN211 failed across all tested concentrations (Fig. 1D), indicating that LN211 may be more appropriate for eliminating undifferentiated iPSCs and isolating iNCCs compared to LN211-E8.

Throughout the differentiation period, the application of CHIR99021 (CHIR), a GSK-3 inhibitor capable of activating the Wnt/β-Catenin pathway with low cytotoxicity [49], was optimized. CHIR has been employed for a variety of objectives, such as somatic cell reprograming [50,51], pluripotency maintenance [52,53], cell growth promotion [54,55] and differentiation induction into specific tissue cells [56–59]. The impact of CHIR on pluripotent stem cells appear to be influenced by multiple factors, including the developmental stage of cell proliferation and differentiation [56,59], and the cell type [60,61]. Therefore, optimizing the application of CHIR is critical regarding timing, concentration and differentiation stage. Previous studies have indicated that induction efficiency varied due to CHIR concentrations for induction into iNCCs [16]. In this experiment, it was determined that 0.6 μM was

optimal for 201B7 cell line (Fig. 1C). Furthermore, when differentiation induction with other cell lines (1210B2 and 1231A3) was performed under the 0.6 μM CHIR condition, the induction efficiency of 1210B2 and 1231A3 was lower than that of 201B7 (Fig. 1G, Pre purification). This implies that 0.6 μM was optimal for 201B7, and the ideal CHIR concentration might be dependent on the iPSC cell line. After differentiated cells were cultured on LN211 (Fig. 1G, Post purification), the proportion of CD271high cells significantly increased among all cell lines, suggesting that LN211 could serve as a strong scaffold to isolate iNCCs irrespective of cell lines. Moreover, more than 90% iNCCs could be achieved in a single culture passage when LN211 was used as a scaffold for purified culture of iNCCs, regardless of CHIR concentrations (Fig. 1E). Given these results, the innovative method developed in this study for obtaining iNCCs with high efficiency using LN211 is a technique-independent method with no human variability, potentially contributing to a stable supply for cell therapy. While VN and LN511-E8 presented a high CD271high population in several concentrations, these scaffolds also adhere iPSCs [45,62], hence they were deemed unsuitable for iNCC purification.

The objective of this study was to ascertain whether the CD271high cells, designated here as iNCCs, exhibit the characteristics of NCCs. The gene expression patterns of the cells in the first passage of purification culture suggested that the iNCCs closely resembled the migrating NCCs of the first and second pharyngeal arches (Fig. 2B and C). Previous reports have proposed that CHIR can facilitate differentiation into hindbrain NCCs by inhibiting OTX2 expression [63], and steering cells towards cranial or trunk identity in a dose-dependent manner [64]. In this study, OTX2 expression at the end of induction was low in a CHIR concentration-dependent manner in the induction medium (Fig. S1 A), indicating that CHIR in the iNCC induction medium may play a substantial role in determining the type of iNCCs. At the conclusion of CD271high cells induction, the mesencephalic NCC marker and the first, second, and third pharyngeal arch marker genes were expressed. However, in the first culture passage of purification culture, only Dlx1, the marker for first and second pharyngeal arches, was highly expressed (Fig. S1 B), while the expression of other marker genes was notably reduced (Fig. S1 A, C, D). These findings suggest that while the induction method for CD271high cells utilized in this study generates head NCC-like cells from various sites, a purified culture with LN211 may enrich iNCCs with characteristics of the first and second pharyngeal arch.

The iNCCs acquired using LN211 also displayed self-renewal and multipotency, which are characteristics of NCCs. The iNCCs could be cultured on LN211 for 13 passages (approximately 57 days) or longer while maintaining CD271high profiles (Fig. 2A), suggesting that LN211 is suitable not only for purification but also for subsequent growth maintenance culture of iNCCs. It is recognized that SOX10 and SOX9 play a role in regulating the differentiation of NCCs [65,66]. Moreover, it is known that NCCs of the first and second pharyngeal arches possess the ability to differentiate into various cell types, including neurons, Schwann cells, melanocytes, smooth muscle cells, osteoblasts, adipocytes and chondrocytes [7,67]. As previous studies have demonstrated, the iNCCs with gene expression patterns similar to those observed in this study can differentiate into these cell types [16]. The iNCCs in this study exhibited high levels of gene expression for both SOX9 and SOX10 (Fig. 1E) and demonstrated the ability to differentiate into each of the aforementioned tissues (Fig. 2D). These findings regarding the self-renewal and multipotency of iNCCs procured with LN211 suggest their potential as a source for cell therapy, providing the necessary quantities and cell types.

Mesenchymal stem cells (MSCs) are among the most promising cellular therapeutics, being employed in various therapies such as graft-versus-host disease (GvHD), cardiovascular disease, neurodegenerative and orthopedic diseases [68]. To overcome donor limitations, various groups have attempted to induce iMSCs from iPSCs [16,69,70], and multiple groups have reported that iNCCs could be differentiated into iMSCs, serving as intermediate cells for cell therapy sources. The iMSCs derived from iNCCs obtained in this study exhibited MSC surface marker expression (Fig. 3B) and differentiation ability (Fig. 3C). Furthermore, the cells obtained demonstrated limited cell proliferation (Fig. 3A), suggesting the acquisition of iMSCs with features comparable to somatic MSCs. MSCs are known to sense inflammatory sites in vivo and inhibit the function of activated T cells by producing IDO, among other factors [71,72]. Such immunosuppressive properties are therefore anticipated to have therapeutic effects on refractory diseases such as GvHD. In the iMSCs obtained, similar to somatic BM-MSCs, the protein expression of IDO was upregulated upon IFNγ stimulation (Fig. 3D), indicating the suppression of proliferation of activated PBMCs via an IDO-mediated mechanism (Fig. 3E). These results suggest that iNCCs procured with LN211 might be beneficial as intermediate cells for producing iMSCs for cell therapy.

5. Conclusion

This study aimed to overcome the constrains of conventional methods by establishing a straightforward, cost-effective, and highly efficient procedure for producing iNCCs from iPSCs with a brief culture period. This is the first instance where LN211 has been employed as a purification scaffold material to isolate iNCCs from heterogeneous cell populations, enabling the high-efficiency purification of iNCCs without the necessity for expensive equipment such as FACS or long-term passage. The iNCCs obtained via this method retained CD271high profiles even after more than ten passages and successfully differentiated into various cell types. Furthermore, the induction of iMSCs from these iNCCs was confirmed, displaying properties akin to BM-MSCs. These results suggest that this newly established method could contribute to the stable supply of iNCCs, thereby paving the way for future cell therapies.

Declaration of Generative AI and AI-assisted technologies in the writing process

During the preparation of this work the author used OpenAI's language model, GPT-4, in order to assist with language editing and improving readability of the manuscript. After using this tool, the author reviewed and edited the content as needed and takes full responsibility for the content of the publication.

Conflict of interest

We hereby declare that there are no conflicts of interest to report. We confirm that there have been no financial or personal relationships with other people or organizations that could inappropriately influence or bias our work.

Acknowledgements

for his insightful advice on the characteristics and properties of induced neural crest cells.

Appendix A. Supplementary data

Supplementary data to this article can be found online at https://doi.org/10.1016/j.reth.2024.08.024.

References

[1] Thomson JA, Itskovitz-Eldor J, Shapiro SS, Waknitz MA, Swiergiel JJ, Marshall VS, et al. Embryonic stem cell lines derived from human blastocysts. Science 1998;282(80-):1145–7. https://doi.org/10.1126/science.282.5391.1145.

[2] Takahashi K, Tanabe K, Ohnuki M, Narita M, Ichisaka T, Tomoda K, et al. Induction of pluripotent stem cells from adult human fibroblasts by defined factors. Cell 2007;131:861–72. https://doi.org/10.1016/j.cell.2007.11.019.

[3] Matsumoto Y, Ikeya M, Hino K, Horigome K, Fukuta M, Watanabe M, et al. New protocol to optimize iPS cells for genome analysis of fibrodysplasia ossificans progressiva. Stem Cell 2015;33:1730–42. https://doi.org/10.1002/stem.1981.

[4] Mandai M, Watanabe A, Kurimoto Y, Hirami Y, Morinaga C, Daimon T, et al. Autologous induced stem-cell–derived retinal cells for macular degeneration. N Engl J Med 2017;376:1038–46. https://doi.org/10.1056/NEJMoa1608368.

[5] Liu Z, Tang Y, Lü S, Zhou J, Du Z, Duan C, et al. The tumourigenicity of iPS cells and their differentiated derivates. J Cell Mol Med 2013;17. https://doi.org/10.1111/jcmm.12062.

[6] Le Douarin NM, Dupin E. Multipotentiality of the neural crest. Curr Opin Genet Dev 2003;13. https://doi.org/10.1016/j.gde.2003.08.002.

[7] Sauka-Spengler T, Bronner-Fraser M. A gene regulatory network orchestrates neural crest formation. Nat Rev Mol Cell Biol 2008;9:557–68. https://doi.org/10.1038/nrm2428.

[8] Hall BK. The neural crest as a fourth germ layer and vertebrates as quadroblastic not triploblastic. Evol Dev 2000;2. https://doi.org/10.1046/j.1525-142X.2000.00032.x.

[9] Kalcheim C. Mechanisms of early neural crest development: from cell specification to migration. Int Rev Cytol 2000;200. https://doi.org/10.1016/s0074-7696(00)00004-8.

[10] Le Douarin NM, Kalcheim C. The neural crest. Cambridge: Cambridge University Press; 1999.

[11] Nagoshi N, Shibata S, Kubota Y, Nakamura M, Nagai Y, Satoh E, et al. Ontogeny and multipotency of neural crest-derived stem cells in mouse bone marrow, dorsal root ganglia, and whisker pad. Cell Stem Cell 2008;2. https://doi.org/10.1016/j.stem.2008.03.005.

[12] Kruger GM, Mosher JT, Bixby S, Joseph N, Iwashita T, Morrison SJ. Neural crest stem cells persist in the adult gut but undergo changes in self-renewal, neuronal subtype potential, and factor responsiveness. Neuron 2002;35. https://doi.org/10.1016/S0896-6273(02)00827-9.

[13] Liu JA, Cheung M. Neural crest stem cells and their potential therapeutic applications. Dev Biol 2016;419. https://doi.org/10.1016/j.ydbio.2016.09.006.

[14] Stemple DL, Anderson DJ. Isolation of a stem cell for neurons and glia from the mammalian neural crest. Cell 1992;71. https://doi.org/10.1016/0092-8674(92)90393-Q.

[15] Morikawa S, Mabuchi Y, Niibe K, Suzuki S, Nagoshi N, Sunabori T, et al. Development of mesenchymal stem cells partially originate from the neural crest. Biochem Biophys Res Commun 2009;379. https://doi.org/10.1016/j.bbrc.2009.01.031.

[16] Fukuta M, Nakai Y, Kirino K, Nakagawa M, Sekiguchi K, Nagata S, et al. Derivation of mesenchymal stromal cells from pluripotent stem cells through a neural crest lineage using small molecule compounds with defined media. PLoS One 2014;9:1–25. https://doi.org/10.1371/journal.pone.0112291.

[17] Liu Q, Spusta SC, Mi R, Lassiter RNT, Stark MR, Höke A, et al. Human neural crest stem cells derived from human ESCs and induced pluripotent stem cells: induction, maintenance, and differentiation into functional Schwann cells. Stem Cells Transl Med 2012;1. https://doi.org/10.5966/sctm.2011-0042.

[18] Chimge NO, Bayarsaihan D. Generation of neural crest progenitors from human embryonic stem cells. J Exp Zool Part B Mol Dev Evol 2010;314 B. https://doi.org/10.1002/jez.b.21321.

[19] Milet C, Monsoro-Burq AH. Embryonic stem cell strategies to explore neural crest development in human embryos. Dev Biol 2012;366. https://doi.org/10.1016/j.ydbio.2012.01.016.

[20] Serrano F, Bernard WG, Granata A, Iyer D, Steventon B, Kim M, et al. A novel human pluripotent stem cell-derived neural crest model of treacher collins syndrome shows defects in cell death and migration. Stem Cells Dev 2019;28:81–100. https://doi.org/10.1089/scd.2017.0234.

[21] Menendez L, Yatskievych TA, Antin PB, Dalton S. Wnt signaling and a Smad pathway blockade direct the differentiation of human pluripotent stem cells to multipotent neural crest cells. Proc Natl Acad Sci 2011;108:19240–5. https://doi.org/10.1073/pnas.1113746108.

[22] Mica Y, Lee G, Chambers SM, Tomishima MJ, Studer L. Modeling neural crest induction, melanocyte specification, and disease-related pigmentation defects in hESCs and patient-specific iPSCs. Cell Rep 2013;3. https://doi.org/10.1016/j.celrep.2013.03.025.

[23] Kamiya D, Takenaka-Ninagawa N, Motoike S, Kajiya M, Akaboshi T, Zhao C, et al. Induction of functional xeno-free MSCs from human iPSCs via a neural crest cell lineage. Npj Regen Med 2022;7:1–2. https://doi.org/10.1038/s41536-022-00241-8.

[24] Miyazaki T, Isobe T, Nakatsuji N, Suemori H. Efficient adhesion culture of human pluripotent stem cells using laminin fragments in an uncoated manner. Sci Rep 2017;7:1–8. https://doi.org/10.1038/srep41165.

[25] Lai X, Liu J, Zou Z, Wang Y, Wang Y, Liu X, et al. SOX10 ablation severely impairs the generation of postmigratory neural crest from human pluripotent stem cells. Cell Death Dis 2021;12. https://doi.org/10.1038/s41419-021-04099-4.

[26] Shibata S, Hayashi R, Okubo T, Kudo Y, Katayama T, Ishikawa Y, et al. Selective laminin-directed differentiation of human induced pluripotent stem cells into distinct ocular lineages. Cell Rep 2018;25:1668–1679.e5. https://doi.org/10.1016/j.celrep.2018.10.032.

[27] Morrison SJ, White PM, Zock C, Anderson DJ. Prospective identification, isolation by flow cytometry, and in vivo self-renewal of multipotent mammalian neural crest stem cells. Cell 1999;96. https://doi.org/10.1016/S0092-8674(00)80583-8.

[28] Kimura C, Takeda N, Suzuki M, Oshimura M, Aizawa S, Matsuo I. Cis-acting elements conserved between mouse and pufferfish Otx2 genes govern the expression in mesencephalic neural crest cells. Development 1997;124:3929–41. https://doi.org/10.1242/dev.124.20.3929.

[29] Qiu M, Bulfone A, Ghattas I, Meneses JJ, Christensen L, Sharpe PT, et al. Role of the Dlx homeobox genes in proximodistal patterning of the branchial arches: mutations of Dlx-1, Dlx-2, and Dlx-1 and -2 alter morphogenesis of proximal skeletal and soft tissue structures derived from the first and second arches. Dev Biol 1997;185:165–84. https://doi.org/10.1006/dbio.1997.8556.

[30] Manley NR, Capecchi MR. The role of Hoxa-3 in mouse thymus and thyroid development. Development 1995;121:1989–2003. https://doi.org/10.1242/dev.121.7.1989.

[31] Liu Z, Yu S, Manley NR. Gcm2 is required for the differentiation and survival of parathyroid precursor cells in the parathyroid/thymus primordia. Dev Biol 2007;305. https://doi.org/10.1016/j.ydbio.2007.02.014.

[32] Battiwalla M, Hematti P. Mesenchymal stem cells in hematopoietic stem cell transplantation. Cytotherapy 2009;11. https://doi.org/10.1080/14653240903193806.

[33] Galipeau J, Sensébé L. Mesenchymal stromal cells: clinical challenges and therapeutic opportunities. Cell Stem Cell 2018;22. https://doi.org/10.1016/j.stem.2018.05.004.

[34] Mathiasen AB, Qayyum AA, Jørgensen E, Helqvist S, Fischer-Nielsen A, Kofoed KF, et al. Bone marrow-derived mesenchymal stromal cell treatment in patients with severe ischaemic heart failure: a randomized placebo-controlled trial (MSC-HF trial). Eur Heart J 2015;36. https://doi.org/10.1093/eurheartj/ehv136.

[35] Borlongan CV. Concise review: stem cell therapy for stroke patients: are we there yet? Stem Cells Transl Med 2019;8. https://doi.org/10.1002/sctm.19-0076.

[36] Mendicino M, Bailey AM, Wonnacott K, Puri RK, Bauer SR. MSC-based product characterization for clinical trials: an FDA perspective. Cell Stem Cell 2014;14:141–5. https://doi.org/10.1016/j.stem.2014.01.013.

[37] Stenderup K. Aging is associated with decreased maximal life span and accelerated senescence of bone marrow stromal cells. Bone 2003;33:919–26. https://doi.org/10.1016/j.bone.2003.07.005.

[38] Umeda K, Oda H, Yan Q, Matthias N, Zhao J, Davis BR, et al. Long-term expandable SOX9+ chondrogenic ectomesenchymal cells from human pluripotent stem cells. Stem Cell Rep 2015;4:712–26. https://doi.org/10.1016/j.stemcr.2015.02.012.

[39] Menendez L, Kulik MJ, Page AT, Park SS, Lauderdale JD, Cunningham ML, et al. Directed differentiation of human pluripotent cells to neural crest stem cells. Nat Protoc 2013;8:203–12. https://doi.org/10.1038/nprot.2012.156.

[40] Chambers SM, Fasano CA, Papapetrou EP, Tomishima M, Sadelain M, Studer L. Highly efficient neural conversion of human ES and iPS cells by dual inhibition of SMAD signaling. Nat Biotechnol 2009;27. https://doi.org/10.1038/nbt.1529.

[41] Zujur D, Al-Akashi Z, Nakamura A, Zhao C, Takahashi K, Aritomi S, et al. Enhanced chondrogenic differentiation of iPS cell-derived mesenchymal stem/stromal cells via neural crest cell induction for hyaline cartilage repair. Front Cell Dev Biol 2023;11:1–13. https://doi.org/10.3389/fcell.2023.1140717.

[42] Dominici M, Le Blanc K, Mueller I, Slaper-Cortenbach I, Marini F, Krause DS, et al. Minimal criteria for defining multipotent mesenchymal stromal cells. The International Society for Cellular Therapy position statement. Cytotherapy 2006;8:315–7. https://doi.org/10.1080/14653240600855905.

[43] Cimino M, Gonçalves RM, Barrias CC, Martins MCL. Xeno-free strategies for safe human mesenchymal stem/stromal cell expansion: supplements and coatings. Stem Cells Int 2017;2017. https://doi.org/10.1155/2017/6597815.

[44] Fink DW. FDA regulation of stem cell-based products. Science (80-) 2009;324:1662–3. https://doi.org/10.1126/science.1173712.

[45] Hayashi R, Ishikawa Y, Katori R, Sasamoto Y, Taniwaki Y, Takayanagi H, et al. Coordinated generation of multiple ocular-like cell lineages and fabrication of functional corneal epithelial cell sheets from human iPS cells. Nat Protoc 2017;12:683–96. https://doi.org/10.1038/nprot.2017.007.

[46] Ido H, Harada K, Futaki S, Hayashi Y, Nishiuchi R, Natsuka Y, et al. Molecular dissection of the α-Dystroglycan- and integrin-binding sites within the

globular domain of human laminin-10. J Biol Chem 2004;279. https://doi.org/10.1074/jbc.M313626200.

[47] Taniguchi Y, Ido H, Sanzen N, Hayashi M, Sato-Nishiuchi R, Futaki S, et al. The C-terminal region of laminin β chains modulates the integrin binding affinities of laminins. J Biol Chem 2009;284. https://doi.org/10.1074/jbc.M809332200.

[48] Miyazaki T, Futaki S, Suemori H, Taniguchi Y, Yamada M, Kawasaki M, et al. Laminin E8 fragments support efficient adhesion and expansion of dissociated human pluripotent stem cells. Nat Commun 2012;3:1236. https://doi.org/10.1038/ncomms2231.

[49] Naujok O, Lentes J, Diekmann U, Davenport C, Lenzen S. Cytotoxicity and activation of the Wnt/beta-catenin pathway in mouse embryonic stem cells treated with four GSK3 inhibitors. BMC Res Notes 2014;7. https://doi.org/10.1186/1756-0500-7-273.

[50] Li W, Wei W, Zhu S, Zhu J, Shi Y, Lin T, et al. Generation of rat and human induced pluripotent stem cells by combining genetic reprogramming and chemical inhibitors. Cell Stem Cell 2009;4. https://doi.org/10.1016/j.stem.2008.11.014.

[51] Li W, Zhou HY, Abujarour R, Zhu S, Joo JY, Lin T, et al. Generation of human-induced pluripotent stem cells in the absence of exogenous Sox2. Stem Cell 2009;27. https://doi.org/10.1002/stem.240.

[52] Ying QL, Wray J, Nichols J, Batlle-Morera L, Doble B, Woodgett J, et al. The ground state of embryonic stem cell self-renewal. Nature 2008;453. https://doi.org/10.1038/nature06968.

[53] Kiyonari H, Kaneko M, Abe SI, Aizawa S. Three inhibitors of FGF receptor, ERK, and GSK3 establishes germline-competent embryonic stem cells of C57BL/6N mouse strain with high efficiency and stability. Genesis 2010;48. https://doi.org/10.1002/dvg.20614.

[54] Jiang M, Chen H, Lai S, Wang R, Qiu Y, Ye F, et al. Maintenance of human haematopoietic stem and progenitor cells in vitro using a chemical cocktail. Cell Discov 2018;4. https://doi.org/10.1038/s41421-018-0059-5.

[55] Fan Y, Ho BX, Pang JKS, Pek NMQ, Hor JH, Ng SY, et al. Wnt/β-catenin-mediated signaling re-activates proliferation of matured cardiomyocytes. Stem Cell Res Ther 2018;9. https://doi.org/10.1186/s13287-018-1086-8.

[56] Lian X, Bao X, Al-Ahmad A, Liu J, Wu Y, Dong W, et al. Efficient differentiation of human pluripotent stem cells to endothelial progenitors via small-molecule activation of WNT signaling. Stem Cell Rep 2014;3. https://doi.org/10.1016/j.stemcr.2014.09.005.

[57] Mae SI, Shono A, Shiota F, Yasuno T, Kajiwara M, Gotoda-Nishimura N, et al. Monitoring and robust induction of nephrogenic intermediate mesoderm from human pluripotent stem cells. Nat Commun 2013;4. https://doi.org/10.1038/ncomms2378.

[58] Naujok O, Diekmann U, Lenzen S. The generation of definitive endoderm from human embryonic stem cells is initially independent from activin A but requires canonical Wnt-signaling. Stem Cell Rev Reports 2014;10. https://doi.org/10.1007/s12015-014-9509-0.

[59] Gonzalez R, Lee JW, Schultz PG. Stepwise chemically induced cardiomyocyte specification of human embryonic stem cells. Angew Chemie - Int Ed 2011;50. https://doi.org/10.1002/anie.201103909.

[60] Fonoudi H, Ansari H, Abbasalizadeh S, Larijani MR, Kiani S, Hashemizadeh S, et al. A universal and robust integrated platform for the scalable production of human cardiomyocytes from pluripotent stem cells. Stem Cells Transl Med 2015;4. https://doi.org/10.5966/sctm.2014-0275.

[61] Kempf H, Olmer R, Kropp C, Rückert M, Jara-Avaca M, Robles-Diaz D, et al. Controlling expansion and cardiomyogenic differentiation of human pluripotent stem cells in scalable suspension culture. Stem Cell Rep 2014;3. https://doi.org/10.1016/j.stemcr.2014.09.017.

[62] Sung TC, Liu CH, Huang WL, Lee YC, Kumar SS, Chang Y, et al. Efficient differentiation of human ES and iPS cells into cardiomyocytes on biomaterials under xeno-free conditions. Biomater Sci 2019;7. https://doi.org/10.1039/c9bm00817a.

[63] McGrew LL, Lai CJ, Moon RT. Specification of the anteroposterior neural Axis through synergistic interaction of the Wnt signaling cascade withnogginandfollistatin. Dev Biol 1995;172. https://doi.org/10.1006/dbio.1995.0027.

[64] Hackland JOS, Shelar PB, Sandhu N, Prasad MS, Charney RM, Gomez GA, et al. FGF modulates the axial identity of trunk hPSC-derived neural crest but not the cranial-trunk decision. Stem Cell Rep 2019;12:920–33. https://doi.org/10.1016/j.stemcr.2019.04.015.

[65] Lee EM, Yuan T, Ballim RD, Nguyen K, Kelsh RN, Medeiros DM, et al. Functional constraints on SoxE proteins in neural crest development: the importance of differential expression for evolution of protein activity. Dev Biol 2016;418. https://doi.org/10.1016/j.ydbio.2016.07.022.

[66] Meulemans D, Bronner-Fraser M. Gene-regulatory interactions in neural crest evolution and development. Dev Cell 2004;7. https://doi.org/10.1016/j.devcel.2004.08.007.

[67] Bronner-Fraser M, Fraser SE. Cell lineage analysis reveals multipotency of some avian neural crest cells. Nature 1988;335. https://doi.org/10.1038/335161a0.

[68] Lukomska B, Stanaszek L, Zuba-Surma E, Legosz P, Sarzynska S, Drela K. Challenges and controversies in human mesenchymal stem cell therapy. Stem Cells Int 2019;2019:1–10. https://doi.org/10.1155/2019/9628536.

[69] Hynes K, Menicanin D, Mrozik K, Gronthos S, Bartold PM. Generation of functional mesenchymal stem cells from different induced pluripotent stem cell lines. Stem Cells Dev 2014;23:1084–96. https://doi.org/10.1089/scd.2013.0111.

[70] Vodyanik MA, Yu J, Zhang X, Tian S, Stewart R, Thomson JA, et al. A mesoderm-derived precursor for mesenchymal stem and endothelial cells. Cell Stem Cell 2010;7:718–29. https://doi.org/10.1016/j.stem.2010.11.011.

[71] Chao YH, Lin CW, Pan HH, Yang SF, Weng TF, Peng CT, et al. Increased apoptosis and peripheral blood mononuclear cell suppression of bone marrow mesenchymal stem cells in severe aplastic anemia. Pediatr Blood Cancer 2018;65. https://doi.org/10.1002/pbc.27247.

[72] Benvenuto F, Voci A, Carminati E, Gualandi F, Mancardi G, Uccelli A, et al. Human mesenchymal stem cells target adhesion molecules and receptors involved in T cell extravasation. Stem Cell Res Ther 2015;6. https://doi.org/10.1186/s13287-015-0222-y.